

Hydrophobic Sponge for Spilled Oil Absorption

Lei Peng, Shuai Yuan, Ge Yan, Ping Yu, Yunbai Luo

College of Chemistry and Molecular Sciences, Wuhan University, Wuhan 430072, China

Correspondence to: Y. Luo (E-mail: ybai@whu.edu.cn)

ABSTRACT: As the ecological damage caused by marine oil spills has become one main threat to marine ecological security, materials that can reduce environmental pollution are in high demand. In this study, a simple low-cost method for fabricating a hydrophobic polyurethane sponge was investigated. Its hydrophobicity was evaluated through the measurement of the contact angles of water and oil. The mechanical properties, oil-absorption capacity, and selectivity were also tested. The results show that this sponge exhibited good mechanical properties, a high absorption capacity and selectivity, and a high reusability (>200 times) in oil–water separation. More importantly, the absorbed oil could be collected by simple squeezing. © 2014 Wiley Periodicals, Inc. *J. Appl. Polym. Sci.* **2014**, *131*, 40886.

KEYWORDS: crosslinking; coatings; foams; recycling; surfaces and interfaces

Received 22 December 2013; accepted 17 April 2014

DOI: 10.1002/app.40886

INTRODUCTION

Crude oil leakage during oil tanker sinking or industrial accidents is catastrophic for marine and aquatic ecosystems.¹ The cleanup of spilled crude oil from the sea has been a major environmental issue, and great efforts have been made to search for effective cleaning methods. Available techniques have been applied to clean oil; these include physical absorption by absorbent materials, mechanical cleaning by oil skimmers, burning, physical diffusion, and biodegradation.^{2–6} Among them, absorbent materials have attracted broad attention because of their simple, efficient, and fast countermeasures for the cleanup of oil spills.^{7–10} Zhang et al.¹¹ fabricated a kind of superhydrophobic textile for water–oil separation based on a drop-coating route. Hayase et al.¹ prepared a polymethylsilsesquioxane aerogel by a sol–gel process for oil absorption. Zhang et al.¹⁰ prepared a kind of multifunctional foam for oil–water separation.¹⁰ Recently, superhydrophobic graphene-based materials were prepared for the separation of water and oil. Nguyen et al.¹² fabricated a graphene-based sponge by a facile dip-coating method. However, oil absorption by these absorbent materials, such as fibers, aerogels, and nanomaterials, have not been as good in practice. Fibers have the limitations of low reusability and poor absorption capacity.^{11,13,14} Aerogels are susceptible to fracturing under squeezing when high-viscosity oils are absorbed; this reduces their reusability in this situation.^{15–18} In addition, their absorption capacities for oils are not considerable.¹ In fact, nanomaterials have some excellent properties, including a high absorption capacity and selectivity.^{12,19–21} However, their preparations almost require intricate equipment or complicated multistep syntheses. Thus, it is not cost-effective to industrialize

them because of their high cost. Therefore, a kind of practical and efficient material for oil absorption and removal is needed.

In this study, we prepare a modified polyurethane (PU) sponge through a simple immersion method that did not require intricate equipment or synthesis processes. The PU sponges showed outstanding capacities with a high absorption capacity, low cost, and good elasticity.^{8,22–28} However, they absorbed not only oil but also water, which greatly weakened their oil-absorption capacity. Here, we anchored hydrophobic trimethylchlorosilane (TMCS)/tetraethoxysilane (TEOS) coatings onto the frames of the sponges to change their wettability. The modified sponges showed a high hydrophobicity, and they absorbed a variety of oils with a high absorption capacity and selectivity. Moreover, the absorbed oil could be removed and collected just by simple squeezing, and then, the sponges could be used again. This ability will not only reduce the cost of spilled oil cleanup but also prevent secondary pollution.

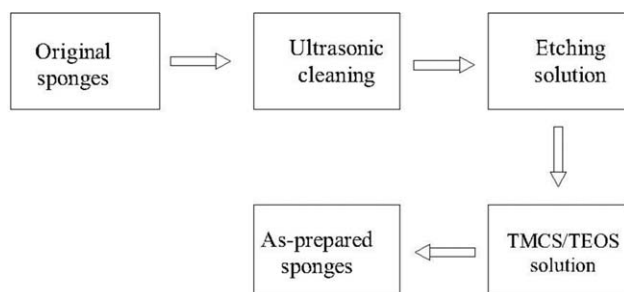
EXPERIMENTAL

Materials

The PU sponges were obtained from a local store. TMCS and TEOS were purchased from Aladdin Reagent Co., Ltd. (Shanghai, China). Acetone, *n*-hexane, sodium chloride, potassium dichromate, and concentrated sulfuric acid were purchased from Sinopharm Chemical Reagent Co., Ltd. (Shanghai, China). All of the chemicals were analytical grade and were used without any further treatment.

Sample Preparation

The PU sponges were cleaned ultrasonically with acetone and distilled water successively to remove possible impurities. After they were etched in chromic acid for 30 s, the PU sponges were



Scheme 1. Preparation procedures of the as-prepared sponges.

washed with distilled water three times and dried at 60°C for 2 h. Then, the pretreated sponges were immersed in an *n*-hexane solution containing TMCS (4% v/v) and TEOS (1% v/v) for 1 h. Then, they were taken out in a humid environment at ambient temperature for 10 h. Finally, the modified sponges were obtained after being dried at 60°C for 2 h. The preparation procedures are shown in Scheme 1. The hydrolysis and polymerization of TMCS and TEOS are shown in Scheme 2.

Characterization

Scanning electron microscopy (SEM) images were obtained by an FEI Quanta 200 (FEI, Holland). The hydrophobicity of the sponges were evaluated by their contact angles, and these were measured by a DSA 100 (Kruss, Germany) with a droplet (10 μ L) of water or crude oil. The mechanical properties of the sponges were measured by an electromechanical universal testing machine CMT6035 (MTS Systems Co., China) with repeated compression processes. The oil-absorption capacities of the sponges were measured by weight measurements at ambient temperature. The water-absorption capacities under different amounts of oil in different salt waters were also measured by weight measurement. The separation of the oil and water were carried out by simple squeezing.

RESULTS AND DISCUSSION

Mechanism of Oil Absorption

Figure 1 shows different magnifications of the SEM images of the PU sponges before and after treatment. Clearly, the surfaces

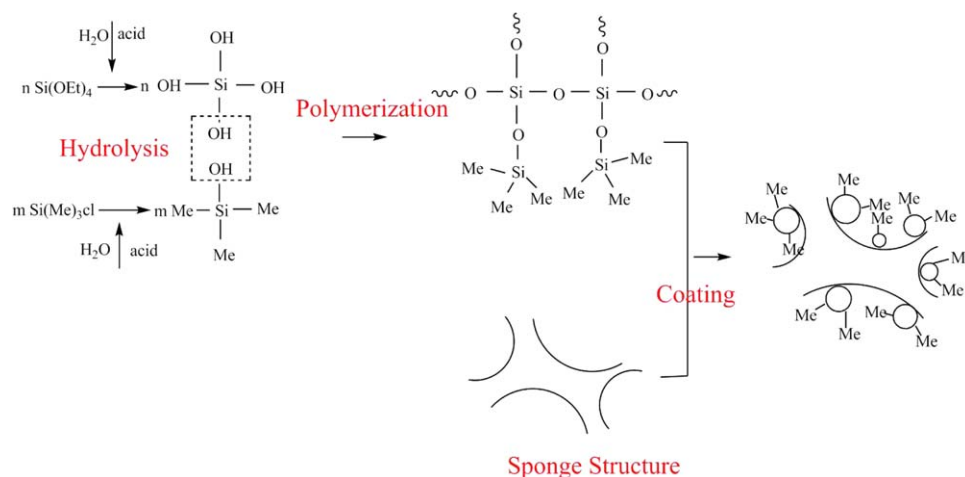
of the untreated PU sponges were smooth and flat [Figure 1(a,b)]. There were no obvious microscale protrusions or spherical structures distributed on the surfaces in the low-magnification [Figure 1(a)] and high-magnification [Figure 1(b)] SEM images. In contrast, the surface of the treated sponge exhibited random roughness, as indicated in the low-magnification SEM image in Figure 1(c). Moreover, many tiny spherical particles were distributed on the sponge, as indicated by the high-magnification SEM image in Figure 1(d).

The SEM images demonstrated that treatment with the silane coupling agent (TMCS and TEOS) resulted in the formation of spherical particles on the surface. The spherical particles were very important to the hydrophobicity of the sponges, just like surface protrusions to the hydrophobicity of lotus leaves.²⁹ Moreover, these spherical particles were a key reason for the spontaneous absorption of oil. As shown in Figure 1(d), there were dense interspaces between different spherical particles. These interspaces could be considered as many tiny capillaries,^{30–32} and the additional pressure (ΔP) of the capillaries could be calculated by the capillary model [Figure 1(e)]. ΔP was derived from the Laplace equation:

$$\Delta P = \frac{2\gamma}{r_1}, \quad \cos \theta = r/r_1$$

where γ is the interfacial tension of oil (~ 28 mN/m); θ is the contact angle between the oil and the spherical particles; and r_1 and r are the radius of curvature and the mean radius of the interspaces [~ 0.2 μ m from Figure 1(d)], respectively; and $\Delta P = 5.6 \times 10^5 \cos \theta$ (Pa). As θ was very small, even close to 0° [shown later in Figure 3(c)], ΔP was close to 5.6×10^5 Pa. This high ΔP was the main reason why the oil could be absorbed in seconds.

Energy-dispersive spectrometry analysis was also used to prove the surface modification (Figure 2). The treated sponge showed a peak of silicon in the energy-dispersive spectrometry analysis [Figure 2(b)]; however, the original one showed no peak of silicon [Figure 2(a)]. This meant that the silane coupling agent was anchored onto the surface of the treated sponge.



Scheme 2. Hydrolysis and polymerization of TMCS and TEOS. [Color figure can be viewed in the online issue, which is available at wileyonlinelibrary.com.]

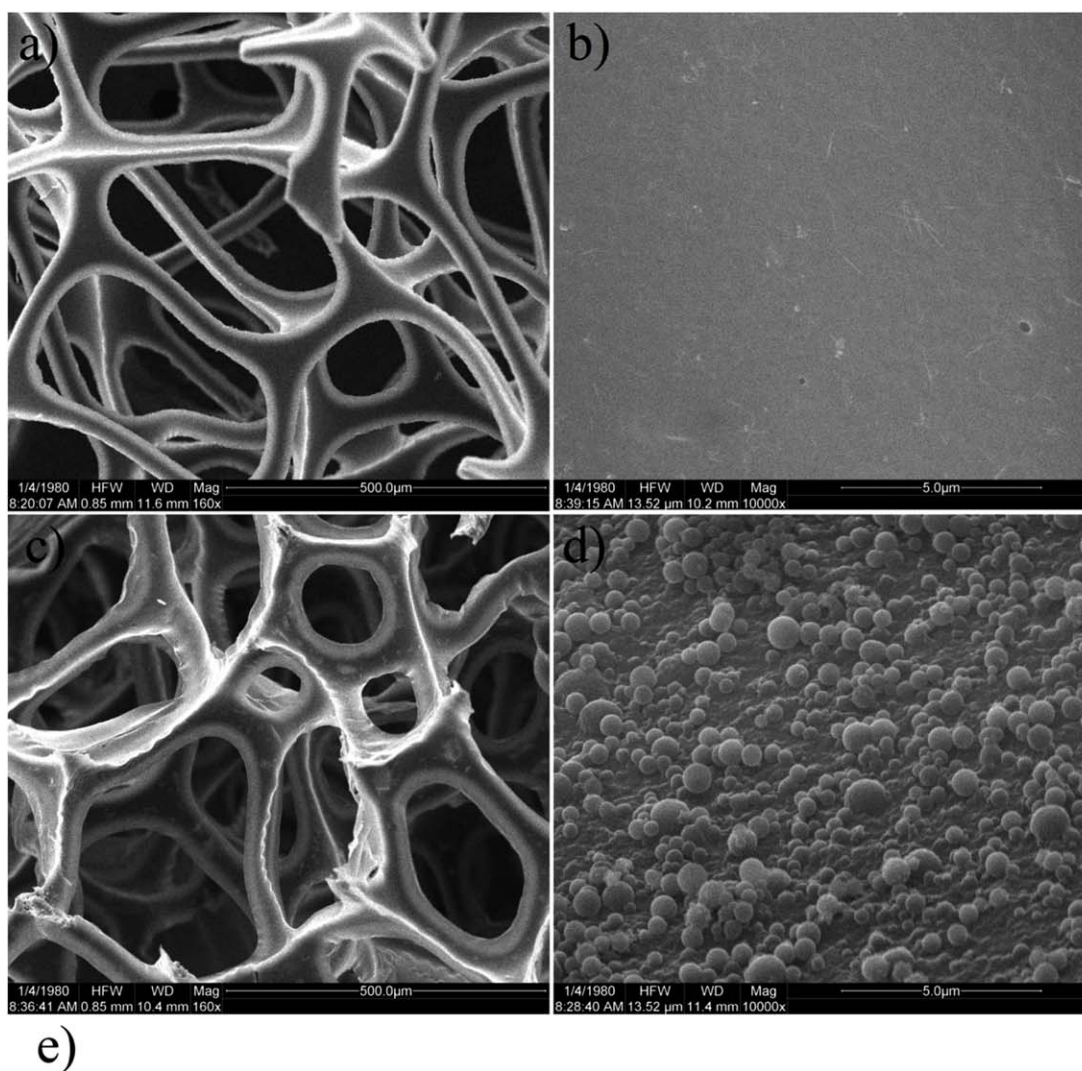


Figure 1. SEM images of the PU sponges (a,b) before and (c,d) after treatment at different magnifications. (e) Interspaces between different spherical particles in the capillary model. [Color figure can be viewed in the online issue, which is available at wileyonlinelibrary.com.]

Contact Angles

The hydrophilicity and hydrophobicity of the sponges were estimated by the measurement of the contact angles.^{8,22–25} The contact angles of the modified and unmodified PU sponges are shown in Figure 3. As shown in Figure 3(a), the water contact angle of the sponge without modification was about 64° ; this showed its intrinsic hydrophilicity. However, after modification,

the water contact angle was enlarged to 137° [Figure 3(b)]. The increase in the contact angle was attributed to the polymerization of the silane coupling agent (TEOS or TMCS); this not only increased the surface roughness but also anchored hydrophobic group ($-\text{CH}_3$) onto the structure of the sponge. As shown in Figure 3(b), the water droplet stood on the sponge surface with the shape of a sphere rather than permeating into

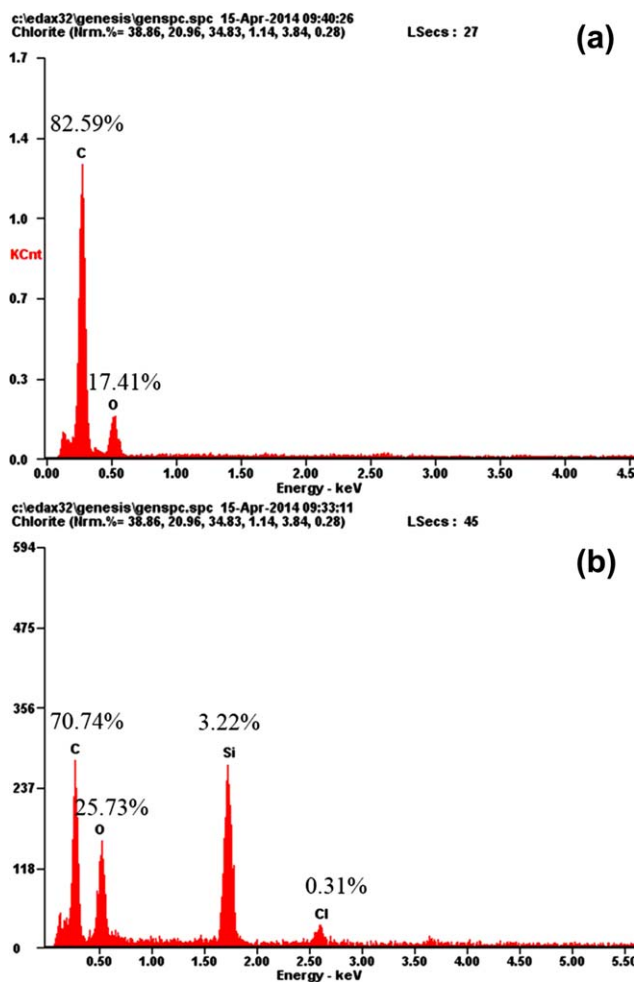


Figure 2. Energy-dispersive spectrometer analyses of the original sponge and the treated sponge. [Color figure can be viewed in the online issue, which is available at wileyonlinelibrary.com.]

the sponge or spreading on the surface, although there were abundant protruding structures on the surface. As shown in Figure 3(c), an oil droplet permeated into the as-prepared sponge rapidly in less than 1 s, and the oil contact angle could not be measured; this showed the good lipophilic properties of the treated sponges. Water droplets (at pH = 1, 14, and 7) could easily stand on the surface of the treated sponge with a spherical shape [Figure 3(d)].

The reasons why the water droplets stood on the surface while oil permeated it were related to the Gibbs energy (ΔG). For the spreading process, according to the Gibbs equation

$$\Delta G = \gamma^{ls} + \gamma^l - \gamma^s$$

and Young's equation

$$\gamma^s = \gamma^{ls} + \gamma^l \cos \theta$$

we derived

$$\Delta G = -\gamma^l (\cos \theta - 1)$$

where the superscripts *s* and *l* represented the solid and liquid phases, respectively. With the growth of θ , ΔG increased; this made the spreading of the water droplet harder. When the water

contact angle was as large as 137° , ΔG was greater than 0; this means that water droplets could not spread spontaneously. However, the oil contact angle was very small, even close to 0° . Thus, ΔG was nearly 0, and the oil could spread easily.

Mechanical Properties

The mechanical properties of the as-prepared sponges were evaluated by the measurement of the cyclic stress–strain⁸ (Figure 4), which reflected the structural stability of the sponges during compression. The sponges could sustain a large strain deformation (ca. 80%) under a relatively low stress (ca. 2 kPa). When the pressures disappeared, the sponges recovered to almost their original shape elastically, even after 200 cycles. Therefore, when the treated sponges were used in oil absorption, the absorbed oil could be extruded out of the sponge pores by squeezing, and the sponges could be used repeatedly because of their good elastic properties.

Separation of Oil and Water

It was easy to separate the oil and water [Figure 5(a–e)]. When dipped into the water–oil mixtures, the treated sponge was absorbed the oil in seconds [Figure 5(b)]. The absorbed oil was collected through simple squeezing [Figure 5(c)]. The absorption and squeezing processes were repeated until the oil and water were separated. The used sponge floated on water instead of sinking [Figure 5(d)]. This separation method was more eco-friendly and practical than the reported burning off⁴ or heat-treatment methods.³³

When put into contact with oil, the sponge was spontaneously wetted by the oil [Figure 5(b)]; this was related to capillary action. The sponge consisted of many holes, through which the oil moved upward to a high place. These holes could be considered as approximate capillaries, and the hole structures could be considered the walls of the capillaries [Figure 1(a)]. Under this assumption, the height (H^*) of oil that could be absorbed spontaneously was calculated. According to the Laplace equation

$$\Delta P = \frac{2\gamma}{r^*}$$

the equilibrium equation

$$\Delta P = \rho g H^*$$

and

$$\cos \theta = r/r^*$$

we derived

$$H^* = \frac{2\gamma \cos \theta}{r \rho g}$$

where *r* was the sponge hole radius [$\sim 130 \mu\text{m}$; Figure 1(a)], r^* is the radius of curvature, and ρ is the oil density. *g* is gravitational constant, H^* was about $5.4 \cos \theta$ (cm). As θ was very small, even close to 0° , H^* was close to 5.4 cm. This meant that the oil could move upward spontaneously as high as 5.4 cm.

Absorption Capacities of the Oils

In addition, the absorption capacities of the treated sponges for different kinds of oils were investigated (Figure 6); this was an important criterion for the evaluation of the as-prepared

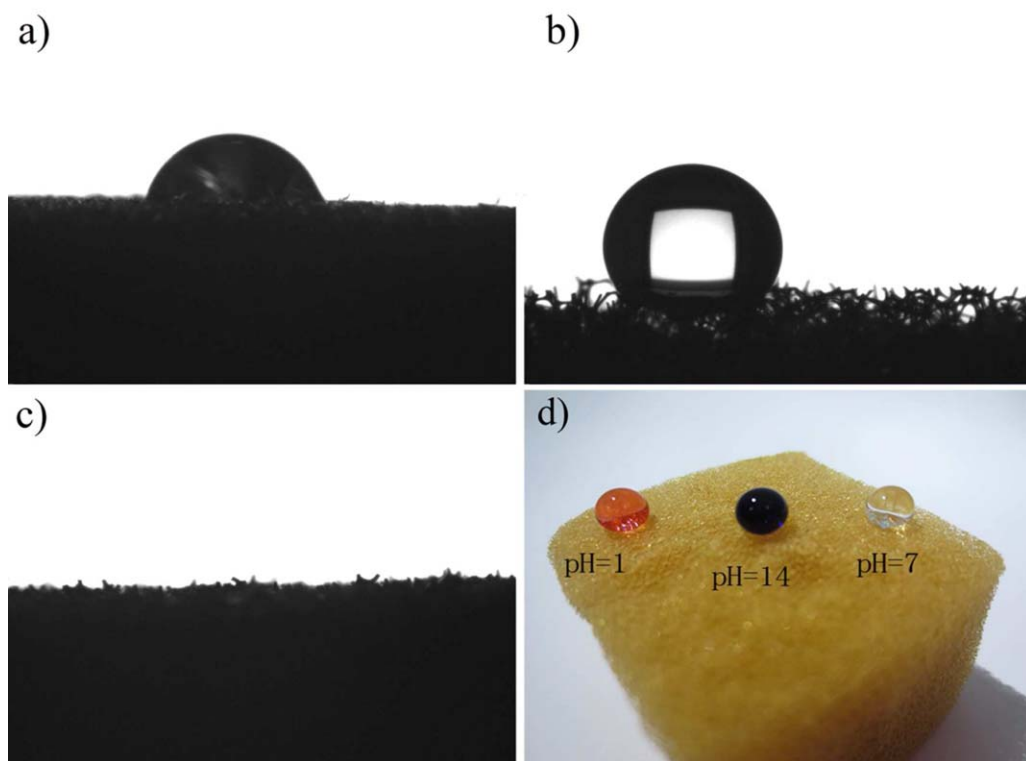


Figure 3. (a) Water contact angle image of the sponge before treatment, (b) water contact angle image of the sponge after treatment, (c) image of the sponge after the crude oil was dropped onto it, and (d) image of water droplets standing on the surface of the treated sponge. [Color figure can be viewed in the online issue, which is available at wileyonlinelibrary.com.]

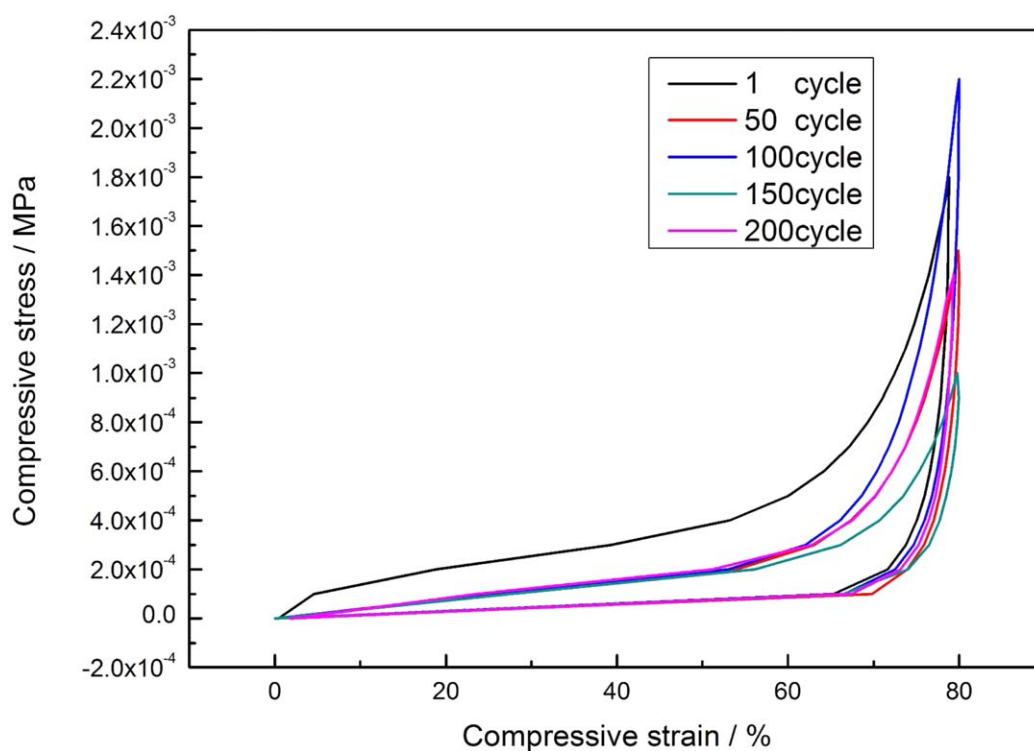


Figure 4. Stress-strain curves of the as-prepared sponges in the process of repeated mechanical compression. [Color figure can be viewed in the online issue, which is available at wileyonlinelibrary.com.]

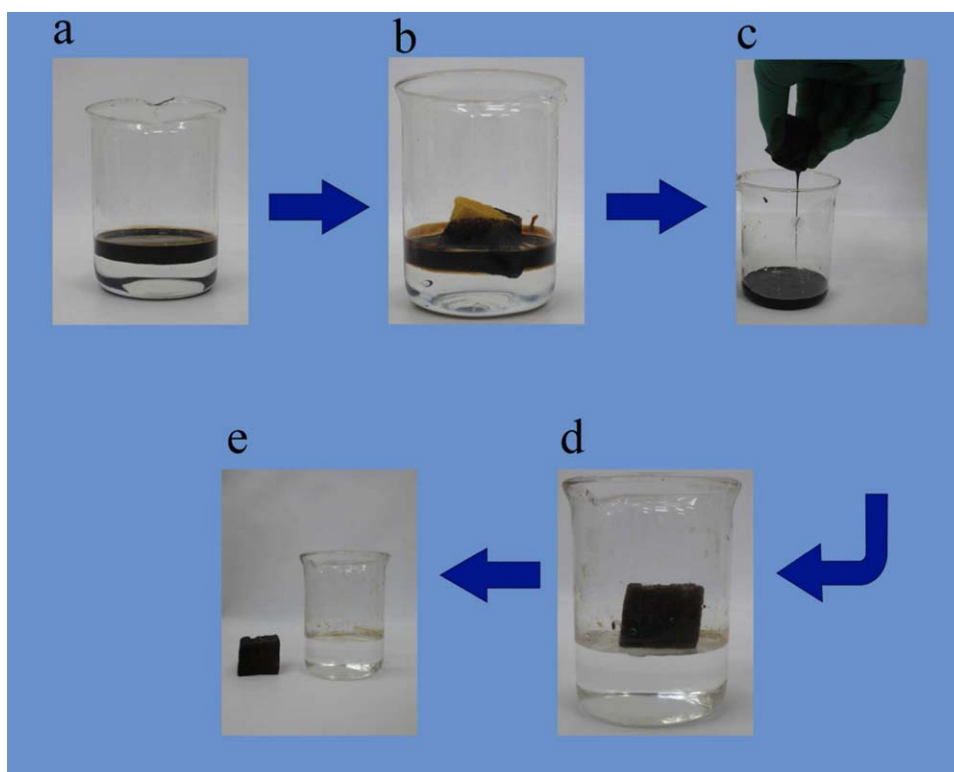


Figure 5. (a–e) Removal and collection of crude oil from the surface of water by the treated sponge. [Color figure can be viewed in the online issue, which is available at wileyonlinelibrary.com.]

sponges.^{10,27} The oil-absorption capacity (k) was measured by weighing methods and was defined as follows:⁷

$$k = (m_{\text{saturated}} - m_{\text{initial}}) / m_{\text{initial}}$$

where $m_{\text{saturated}}$ is the weight of the sponge after oil absorption and m_{initial} is the weight before oil absorption. The high oil-absorption capacity was mainly attributed to the high porosity of the sponges. Oil was stored in the pores via the attractive forces between the oil and the treated sponge.

More importantly, the treated sponges, with their high absorption capacity and efficiency, could be reused; this is an important consideration for practical applications. The absorption capacities with different use times were also investigated to evaluate the reusability (Figure 6). The capacities weakened only slightly after 200 oil-removal cycles; this showed the good reusability of this material. The excellent absorption capacity and reusability could not only reduce the cost of oil-spill cleanup but also save manpower and time.

Selectivity of the Water and Oil

Moreover, the sponge's oil selectivity was also investigated when the amounts of oil were less than its saturated oil capacity (Figure 7). Because of its high lipophilicity, the sponge absorbed oil first. However, when the sponge still had interspaces after the absorption of oil, whether the water would be absorbed in the remaining interspaces was studied. With increasing amounts of oil, the rates of increased mass of the water and sponge were almost the same without obvious up or down trends (Figure 7). This might have been because the increased water adhered to

the surface during absorption. This showed that the sponge did not absorb water, even when there were remaining interspaces. This explained the high oil selectivity of the sponge. In addition, three types of salt water (0, 3.5, and 7.0% salt) were investigated with a concentration of seawater of about 3.5%. There was no obvious difference in absorption between the three types of water; this indicated that the salinity of water was unrelated to the selectivity of the sponge (Figure 7).

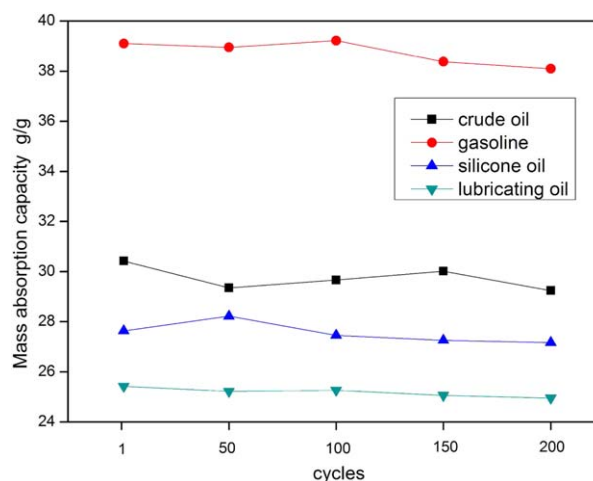


Figure 6. Absorption capacities of the treated sponges for crude oil and other kinds of oils under different cycles. [Color figure can be viewed in the online issue, which is available at wileyonlinelibrary.com.]

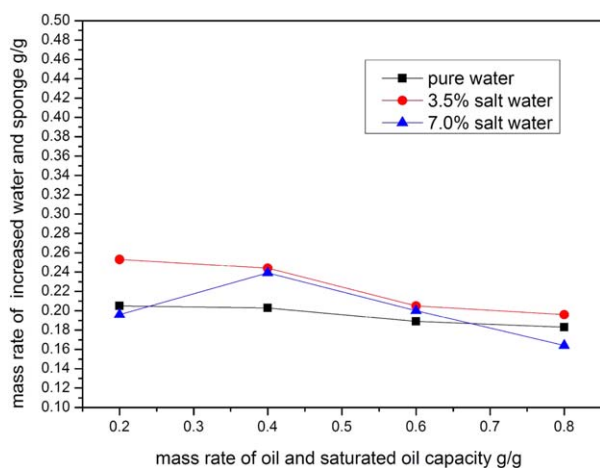


Figure 7. Mass rate of increased water and sponge under different amount of oil in different salty water. [Color figure can be viewed in the online issue, which is available at wileyonlinelibrary.com.]

CONCLUSIONS

We fabricated a hydrophobic PU sponge through a simple immersion method. It was modified by silane coupling agent (TMCS and TEOS) through hydrolysis and polymerization. This sponge showed high hydrophobicity (water contact angle = 137°), high oil-absorption capacity (crude oil \approx 30 g/g), high selectivity (mass rate of increased water and sponge \approx 0.2), and excellent elasticity (with >200 uses). Furthermore, we removed and collected the oil by simple squeezing after the oil was absorbed in the sponge, and then, the sponge could be reused. Because of its good properties, simple method, and low cost, we expected that these treated sponges could be used widely for oil-spill cleanup.

ACKNOWLEDGMENTS

The authors thank the National Science and Technology Support Program (contract grant number 2012BAC02B04).

REFERENCES

- Hayase, G.; Kanamori, K.; Fukuchi, M.; Kaji, H.; Nakanishi, K. *Angew. Chem.* **2013**, *125*, 1.
- Calcagnile, P.; Fragouli, D.; Bayer, I. S.; Anyfantis, G. C.; Martiradonna, L.; Cozzoli, P. D.; Cingolani, R.; Athanassiou, A. *ACS Nano* **2012**, *6*, 5413.
- Broje, V.; Keller, A. A. *J. Hazard. Mater.* **2007**, *148*, 136.
- Aurell, J.; Gullett, B. K. *Environ. Sci. Technol.* **2010**, *44*, 9431.
- Zhao, J.; Xiao, C. F.; Xu, N. K. *J. Dispersion Sci. Technol.* **2012**, *33*, 1197.
- Boopathy, R.; Shields, S.; Nunna, S. *Appl. Biochem. Biotechnol.* **2012**, *167*, 1560.
- Zhou, X.; Zhang, Z.; Xu, X.; Men, X.; Zhu, X. *Ind. Eng. Chem. Res.* **2013**, *52*, 9411.
- Zhu, Q.; Chu, Y.; Wang, Z.; Chen, N.; Lin, L.; Liu, F.; Pan, Q. *J. Mater. Chem. A* **2013**, *1*, 5386.
- Wang, C. F.; Lin, S. J. *ACS Appl. Mater. Interfaces* **2013**, *5*, 8861.
- Zhang, X. Y.; Li, Z.; Liu, K. S.; Jiang, L. *Adv. Funct. Mater.* **2013**, *23*, 2881.
- Zhang, M.; Wang, C.; Wang, S. L.; Li, J. *Carbohydr. Polym.* **2013**, *97*, 59.
- Nguyen, D. D.; Tai, N. H.; Lee, S. B.; Kuo, W. S. *Energy Environ. Sci.* **2012**, *5*, 7908.
- Xue, C. H.; Ji, P. T.; Zhang, P.; Li, Y. R.; Jia, S. T. *Appl. Surf. Sci.* **2013**, *284*, 464.
- Radetić, M. M.; Jocić, D. M.; Jovančić, P. M.; Petrović, Z. L.; Thomas, H. F. *Environ. Sci. Technol.* **2003**, *37*, 1008.
- Sun, H.; Xu, Z.; Gao, C. *Adv. Mater.* **2013**, *25*, 2554.
- Kanamori, K.; Aizawa, M.; Nakanishi, K.; Hanada, T. *Adv. Mater.* **2007**, *19*, 1589.
- Choi, S. J.; Kwon, T. H.; Im, H.; Moon, D. I.; Baek, D. J.; Seol, M. L.; Duarte, J. P.; Choi, Y. K. *ACS Appl. Mater. Interfaces* **2011**, *3*, 4552.
- Wu, Z. Y.; Li, C.; Liang, H. W.; Chen, J. F.; Yu, S. H. *Angew. Chem.* **2013**, *52*, 2925.
- Zhao, Y.; Hu, C. G.; Hu, Y.; Cheng, H. H.; Shi, G. Q.; Qu, L. T. *Angew. Chem.* **2012**, *51*, 11371.
- Cao, A.; Dickrell, P. L.; Sawye, W. G.; Ghasemi-Nejhad, M. N.; Ajayan, P. M. *Science* **2005**, *310*, 1307.
- Yuan, J.; Liu, X.; Akbulut, O.; Hu, J.; Suib, S. L.; Kong, J.; Stellacci, F. *Nat. Nanotechnol.* **2008**, *3*, 332.
- Liang, W. X.; Guo, Z. G. *RSC Adv.* **2013**, *3*, 16469.
- Gui, X.; Cao, A.; Wei, J.; Li, H.; Jia, Y.; Li, Z.; Fan, L.; Wang, K.; Zhu, H.; Wu, D. *ACS Nano* **2010**, *4*, 2320.
- Gui, X.; Wei, J.; Wang, K.; Cao, A.; Zhu, H.; Jia, Y.; Shu, Q.; Wu, D. *Adv. Mater.* **2010**, *22*, 617.
- Wang, C. F.; Lin, S. J. *ACS Appl. Mater. Interfaces* **2013**, *5*, 8861.
- Schaedler, T. A.; Jacobsen, A. J.; Torrents, A.; Sorensen, A. E.; Lian, J.; Greer, J. R.; Valdevit, L.; Carter, W. B. *Science* **2011**, *334*, 962.
- Chen, N.; Pan, Q. M. *ACS Nano* **2013**, *7*, 6875.
- Zhu, L.; Li, C.; Wang, J.; Zhang, H.; Zhang, J.; Shen, Y.; Li, C.; Wang, C.; Xie, A. *Appl. Surf. Sci.* **2012**, *258*, 6326.
- Zhang, Y. L.; Xia, H.; Kim, E.; Sun, H. B. *Soft Matter* **2012**, *8*, 11217.
- Bai, H.; Tian, X.; Zheng, Y.; Ju, J.; Zhao, Y.; Jiang, L. *Adv. Mater.* **2010**, *22*, 5521.
- Tuteja, A.; Choi, W.; Ma, M.; Mabry, J. M.; Mazzella, S. A.; Rutledge, G. C.; McKinley, G. H.; Cohen, R. E. *Science* **2007**, *318*, 1618.
- Zheng, Y.; Bai, H.; Huang, Z.; Tian, X.; Nie, F. Q.; Zhao, Y.; Zhai, J.; Jiang, L. *Nature* **2010**, *463*, 640.
- Gui, X.; Zeng, Z.; Lin, Z. Q.; Gan, Q. M.; Xiang, R.; Zhu, Y.; Cao, A.; Tang, Z. *ACS Appl. Mater. Interfaces* **2013**, *5*, 5845.